The Dynamics of ENSO Anomaly as Revealed in Ensemble Climate Simulations–Impact of Mean Stationary Wave

X.L. Wang,
Climate Prediction Center NCEP / NWS / NOAA, Washington, D.C. 20233

H.L. Rui,
Environmental Modeling Center, NCEP / NWS / NOAA, Washington, D.C. 20233

and *A. Leetmaa*
NCEP / NWS / NOAA, Washington, D.C.20233
Received March 18, 1996; revised May 2, 1996

ABSTRACT

A series of climate ensemble experiments using the climate model from National Centers for Environmental Prediction (NCEP) were performed to exam impact of sea surface temperature (SST) on dynamics of El–Nino / Southern Oscillation (ENSO). A specific question addressed in this paper is how important the mean stationary wave influences anomalous Rossby wave trains or teleconnection patterns as often observed during ENSO events.

Evidences from those ensemble simulations argue that ENSO anomalies, especially over Pacific–North America (PNA) region, appear to be a result of modification for climatological mean stationary wave forced by persistent tropical SST anomalies. Therefore, the role of SST forcing in maintaining climate basic state is emphasized. In this argument, the interaction between atmospheric internal dynamics and external forcing, such as SST is a key element to understand and ultimately predict ENSO.

Key words: ENSO Dynamics, Mean Standing Wave, Tropical–Extratropical Interaction

I. INTRODUCTION

The impact of tropical forcing on low–frequency variability in the extratropics continues to be a key issue as experimental climate prediction is rapidly gaining momentum. Relationships between tropical SST anomalies and extratropical circulation anomalies exist in observations (Bjerknes, 1966, 1969; Horel and Wallace, 1981; van Loon and Madden, 1981; Yarnal and Diaz, 1986; Ropelewski and Halpert, 1987; Kiladis and Diaz, 1989; and many others). However, the relationships are, by no means, conclusive and robust due to contamination by the large natural variability of internal dynamics in extratropics (Kumar and Hoerling, 1995).

During ENSO, wavetrain modes, such as Pacific / North America (PNA), Pacific / South America (PSA), and Tropical / Northern Hemisphere (TNH) patterns, characterize tropical–extratropical teleconnections. In an effort to dynamically explain the wavetrain modes, linear barotropic instability of the zonally asymmetric climatological mean basic state was proposed (Simmons et al., 1983; Branstator, 1985). Other mechanism such as transient eddy forcing (Green, 1977; Kok and Opsteegh, 1983; Shutts, 1986; Hoskins and Sardeshmukh, 1987; Lau, 1988; Held et al., 1989; and many others), and tropical Rossby

wave dispersion (Hoskins and Karoly, 1981; Horel and Wallace, 1981) are also found to be relevant in explaining the wavetrain modes. The extratropical response to tropical forcing depends sensitively on the details of the zonally asymmetric climatological mean basic state (Ting and Sardeshmukh, 1993). An accurate zonally asymmetric climatology is crucial to a model's ability to respond realistically to the anomalous tropical SST forcing (Hoerling et al., 1992; and Ting and Hoerling, 1993). These persuasive evidences point to the importance of zonally asymmetric climatology, i.e., climatological mean stationary wave structure, in understanding the wavetrain modes or tropical–extratropical teleconnection patterns during ENSO and cold events.

In this study, our focus is placed on structural changes of these climatological stationary waves and their relation to tropical SST forcing. Whatever the extratropical response to the tropical SST forcing is, one must also ask how the forcing modifies the natural variability in mid-latitudes. In a recent study of tropical–extratropical interaction, Palmer (1993) and Molteni et al. (1993) have shown that frequency and stability properties of climatological regimes in extratropics can be significantly altered by a strong, persistent SST forcing, such as in ENSO or cold events period. This suggests that SST anomalies in tropics, modifications in the climatological stationary wave in the extratropics, and the preferred occurrence of the wavetrain modes may be well connected to each other during ENSO or cold events when the forcing is strong and persistent. It is our primary interest to shed light on this subject. Our analyses are based on several sets of ensembles of long-term numerical simulations performed using NMC's climate model. A description of the experiments will be presented in Section 2, and a comparison between simulated and observed major features is in Section 3. In Section 4, the importance of climatology in understanding the wavetrains is argued, and evidence to support the argument is presented. The discussion and concluding remarks are found in Section 5.

II. DESCRIPTION OF NUMERICAL EXPERIMENTS

The 500 hPa geopotential heights from several groups of climate simulations and observations were used in this study. The GCM used for these experiments is referred to as MRF9 in Kumar et al. (1994), and a detailed description of the model including its climatology can be found therein.

Three groups of long-term climate simulations were performed, as summarized in Table 1. The first group consists of a nine member ensemble of simulations in which the atmosphere is forced with the monthly mean observed SSTs from Jan. 1969 to Nov. 1993. The simulations were performed first from Feb. 1982 to Nov. 1993. The simulations were performed first from Feb. 1982 to Nov. 1993 for nine ensemble members. With the available of an improved global SST anomalies (Smith, et al., 1995), the simulations were extended back to Jan. 1969. We refer to this group of the simulation, e.g. 1969–1993, as the ensemble, denoted as ENSM. The nine member ensemble mean of the 500 hPa geopotential height is defined as Z_{EM}. The second group consists of a total of five ten-year runs in which the first two, e.g. 20 years of simulation, are forced by climatological SST, designated as $CLIM_{CNTL}$, and the mean of 500 hPa height is Z_{CN}. Then the SST climatology is altered by constantly adding the SST anomaly of Jan. 1992 to all of twelve months to form a warm SST climatology. The third and fourth

simulations, e.g. 20 years of simulation, of this group are forced by the warm SST climatology, $CLIM_{WARM}$, and its 500 hPa mean geopotential height is Z_{CW}. Finally, the last experiment is forced with the cold SST climatology ($CLIM_{COLD}$) which is formed by adding the SST anomaly of Jan. 1989 to each month of the SST climatology, and the 500 hPa height is referred as Z_{CC}. In this group, each of the different initial conditions was selected within the month of Jan. 1982. The third group of simulations consists of three seven-year perpetual simulations forced by observed SST in Jan. 1992 and Jan. 1989, as well as the climatological SST of January, respectively. They are labelled as $PERP_{WARM}$, $PERP_{COLD}$, and $PERP_{CNTL}$, correspondingly. The 500 hPa geopotential heights from this group are labelled as Z_{PW}, Z_{PC}, and Z_{PN}, correspondingly. The symbol Z_{OB} means observation.

Table 1. Ensemble Experiments Performed in This Study

Exp. Group	Exp. Type	Runs	Time	Forcing Field
Ensembles	ENSM	9	69–93	observed SST
Climatology	$CLIM_{CNTL}$	2	10 yrs	Climatological SST
	$CLIM_{WARM}$	2	10 yrs	Clim. SST+SSTa (1 / 92)
	$CLIM_{COLD}$	1	10 yrs	Clim. SST+SSTa (1 / 89)
Perpetual	$PREP_{CNTL}$	1	7 yrs	Clim. Jan. SST
	$PREP_{WARM}$	1	7 yrs	Jan. 1992 SST
	$PREP_{COLD}$	1	7 yrs	Jan. 1989 SST

In order to focus on the zonal asymmetry of simulated climate signal in extratropical latitudes, most of our analysis will be performed on the stationary wave component of the 500 hPa geopotential heights. In the next section, the simulated ENSO anomalies will be analyzed and compared with observations for both the anomalous zonal mean and stationary wave component. Dynamical and physical aspects of simulated climate variations over the Pacific–America sector will be evaluated in Section 4. Since the primary interest of this study is to understand structures and evolutions of climate variability over Pacific and Americal regions, our discussion will focus on features in Pacific / America sector. The discussions and conclusions are in the Section 5.

III. ENSO SIMULATION

1. *Zonal Mean Anomalies*

An important prerequisite for diagnosing climate simulations as a surrogate for observations is that the model be able to reproduce the major climatic features of nature from SST forcing. Therefore, it is important to compare the simulated field with observations. Shown in Fig. 1 are the zonal mean anomalies of Z_{EM} (1a) and Z_{OB} (1b). Before 1979, the observations are only available in the Northern Hemisphere north of 20°N. For several major ENSO events such as 82 / 83, 86 / 87, and 91 / 92, both Z_{EM} and Z_{OB} show positive anomalies in tropics (20°S–20°N) and midlatitudes (poleward of 40°N(S)) and negative anomalies in subtropics (20°N(S)–40°N(S)). The reverse of this pattern is true for cold events, such as

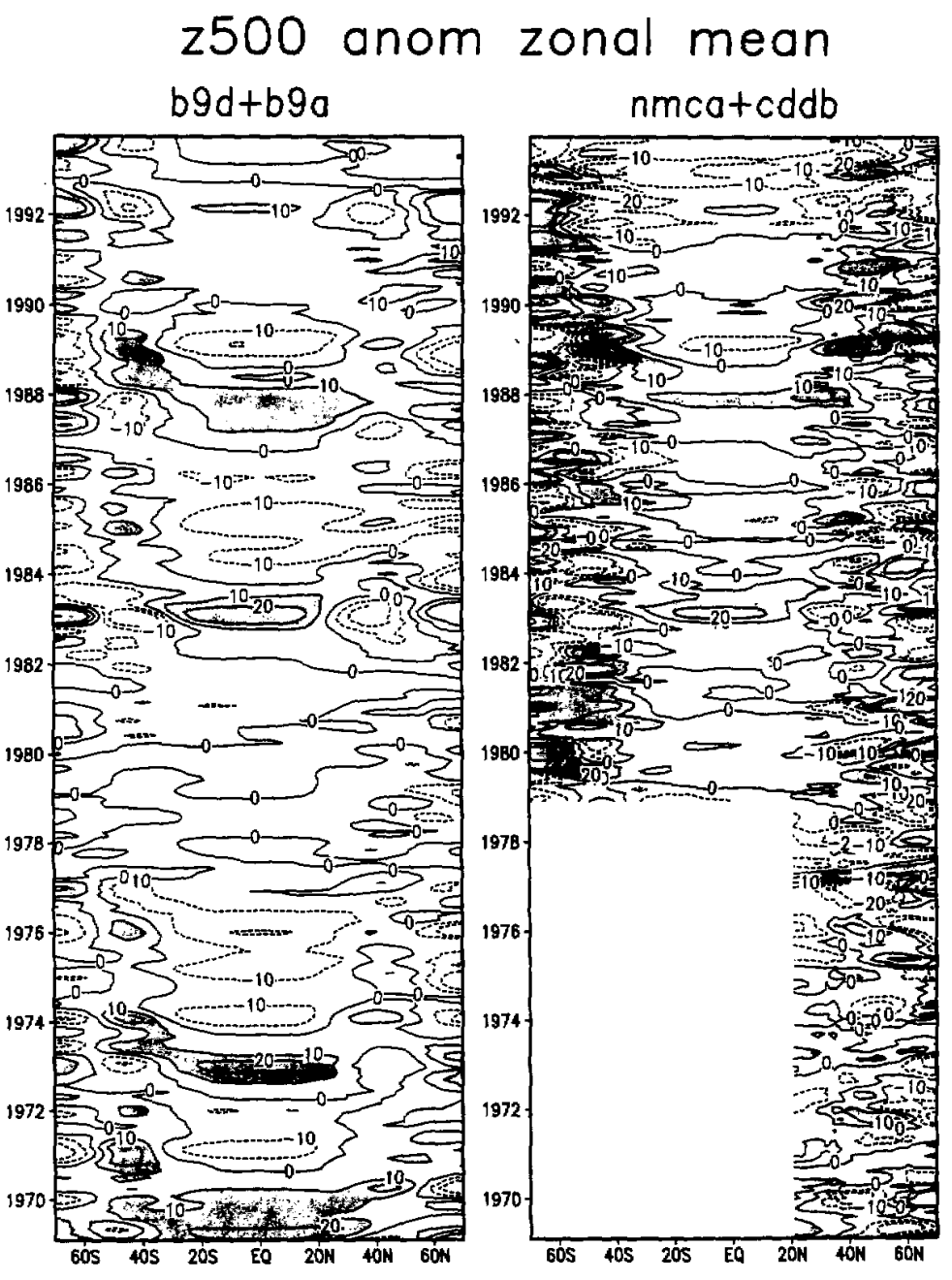

Fig. 1. Anomalous zonal mean of 500 hPa geopotential height for (a) ensemble mean and (b) observation. Intervals are 10m and values greater (less) than 10 (−10) m are dark (light) shaded.

84/85 and 88/89. This is consistent with the results of Dickey et al. (1993) and Rosen (1993). In general, the simulated zonal mean anomalies of Z_{EM} show good agreement to the observations, especially over the tropics. Comparing to the observation, the simulated anomalies are stronger in the tropics and weaker in the extratropics. This difference is not unexpected because the ensemble averaging process enhances signals in the tropics where the direct response to SST forcing and linear dynamics is predominant and diminishes anomalies in extratropics where eddy forcing and non-linear dynamics are major sources of variability.

2. *Stationary Waves*

Over the Western Hemisphere extratropics, wavetrain patterns, such as Pacific/North America (PNA), Pacific/South America (PSA), and Tropical/Northern Hemisphere (TNH), dominate regional climate variability. While these patterns are closely associated with structures of stationary waves, the direct impact of SST anomalies on them is small (Palmer, 1993, Yarnal and Diaz, 1986). However, these are preferred patterns during ENSO events when extratropical eddy forcing associated with stationary wave is changed accordingly.

Shown in Fig. 2 are the first two dominant EOF modes of the model simulated stationary wave of Z_{EM}. They explain about 41 percent of total variance. The first mode (Fig. 2a) describes a wavetrain emanating from the equatorial central Pacific towards midlatitudes in both hemispheres. Hence, it is symmetric with respect to the equator and has an evident tropical origin. From its spatial distribution and temporal evolution (PC1, solid curve of Fig. 2c), it is clear that this mode is associated with anomalous SST forcing during ENSO. The second mode (Fig. 2b) exhibits also a wavetrain structure in extratropics as seen in the first mode, However, there are several fundamental differences between these two modes. Even though the wavetrain structures in individual hemisphere are very similar between two modes, the second mode is antisymmetric with respect to the equator, and has no evidence of tropical origin. Its principal component (PC2, dashed curve of Fig. 2c) contains much higher frequency variations and shows no ENSO signal. A further comparison between PCs of two modes reveals that during ENSO periods wavetrains of both modes tend to reinforce to each other in the Northern (Southern) Hemisphere in winter (summer) and to cancel to each other in the Northern (Southern) Hemisphere in summer (winter). During non-ENSO periods, the second mode dominates.

Observations for global coverage are only available since 1979. Shown in Fig. 3 are the first two EOF modes of observed stationary waves of Z_{OB}. The first mode describes ENSO (PC1, solid curve in Fig. 3c) and is symmetric with respect to the equator (Fig. 3a). Comparing to the simulation (Fig. 2a and 2c), tropical anomalies are relatively weaker in observations. This difference is partially related to ensemble averaging process which maximizes the linear response of SST forcing. The second mode exhibits also antisymmetric spatial structure (Fig. 3b) and higher frequency temporal variation (PC2, dashed curve in Fig. 3c). The Southern Hemisphere wavetrain is ill defined in the observations.

IV. WAVETRAIN DYNAMICS

As mentioned above, anomalous wavetrain tends to be seasonally modulated during ENSO period. However over the extratropics, wavetrains are also evident in non-ENSO

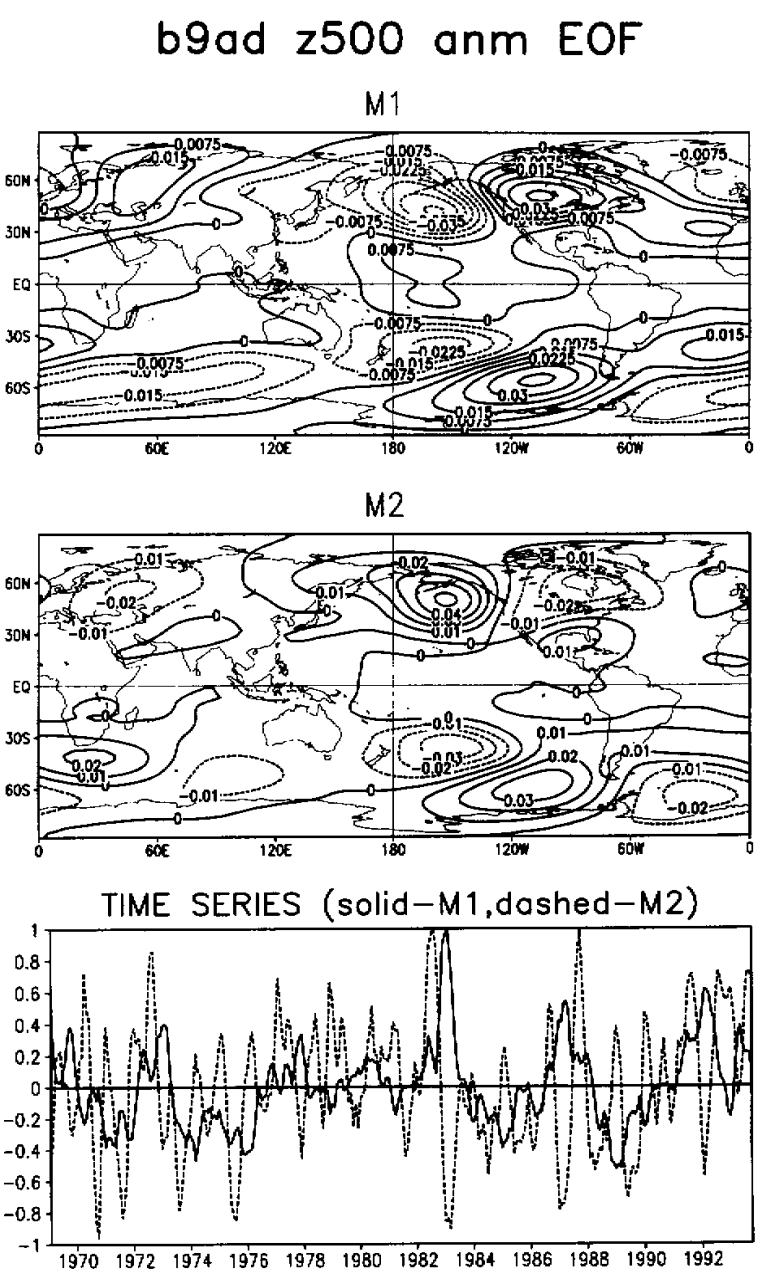

Fig. 2. The first two EOF modes of the 500 hPa eddy geopotential height for the ensemble mean. Interval are 0.0075, the negative values are dashed in (a) and (b). Unit is non−dimensional in all of the EOF plots.

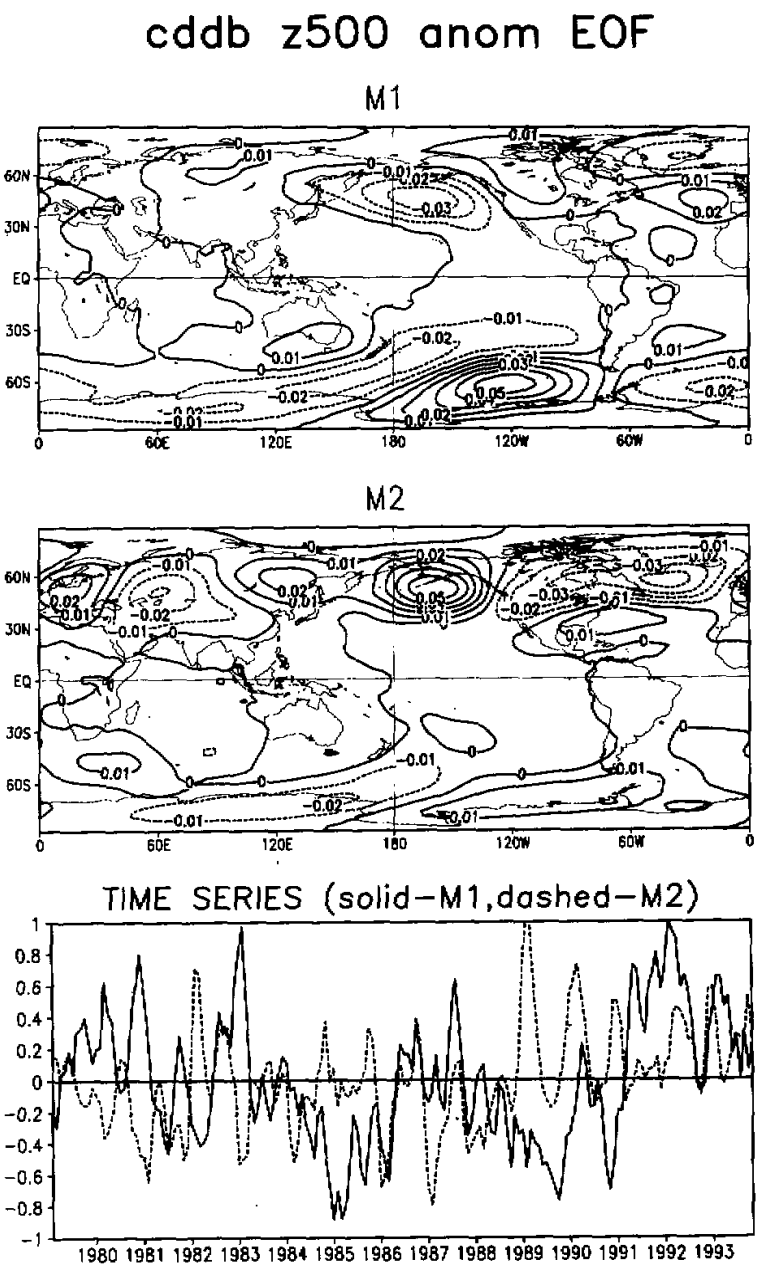

Fig. 3. The first four EOF modes of the 500 hPa eddy geopotential height for observation.

time. Now the questions are: why do these wavetrains predominate during ENSO? What are impacts of SST forcing vs internal dynamics on the wavetrains? Because of the tendency of seasonal modulation of the wavetrains, one may also ask whether there is any relationship between mean climate structures and the wavetrains. While these aspects remain unclear, a series of experiments are performed to explore the nature and dynamics of the wavetrains.

1. *Control Climate Experiments*

The anomalous stationary wave component of the Z_{CN} from two ten-year simulations forced by SST climatology is computed with respect to its own mean seasonal cycle. The first four EOF modes of the stationary wave are shown in Fig. 4. For modes 1 and 2, the strongest spatial loadings are over polar regions (Fig. 4a and 4b). This implies that polar vortex activity dominates variance resulting from internal dynamics. The third and fourth modes (Fig. 4d and 4e) exhibit wavetrain patterns in midlatitudes similar to those in the ensemble simulations. However, the dominant period of those modes (Fig. 4c and 4f) is monthly to sub-seasonal, i.e., much shorter than those in the ensemble simulations. Because there are no SST anomalies in this simulation, the wavetrain patterns seen in Fig. 4d and 4e are solely generated by internal dynamics. These results are consistent with conclusions of Lau (1981).

Although internal dynamics is able to produce these wavetrains in the Pacific / America region, how those relatively higher frequency modes change to the interannual ENSO mode remains unclear. In other words, there has to be a mechanism to persist these wavetrain modes during ENSO in order to change their dominant frequency from monthly and sub-seasonal to interannual. In Fig. 2, we see that the wavetrain patterns show tendency of seasonality and exist during non-ENSO period. This implies that the climatological standing waves of the ensemble simulations and the control experiments may be different and this could possibly influence the wavetrain modes through interaction between anomalous SST forcing and mean stationary waves.

Therefore, anomalous stationary wave component of the Z_{CN} from two ten-year simulations forced by SST climatology is recomputed with respect to the mean seasonal cycle of the Z_{EM}. Show in Fig. 5 is the first EOF mode of this recomputed stationary wave component. Comparing with Fig. 2b, it is obvious that two patterns are very similar. The temporal frequency of corresponding principal component (figure not shown) is also comparable to the PC2 (dashed curve) in Fig. 2c. This illustrates a fact that atmospheric climatology forced by climatological SST differs from one forced with observed SST. The difference between these two type of simulations is anomalous SST forcing. Hence, there is interaction between mean annual cycle and anomalies which is dominated by ENSO variability. In other words, climatological structures of the stationary waves act as a pacemaker for the preferred selection and persistence of the wavetrain modes in the presence of anomalous forcing.

2. *Altered Climate Experiments*

In order to further illustrate the importance of the annual cycle in understanding the physics and dynamics of the wavetrain modes, two SST climatologies were formed by use of SST anomalies in Jan. 1989 and Jan. 1992, respectively. The warm SST climatology is defined as:

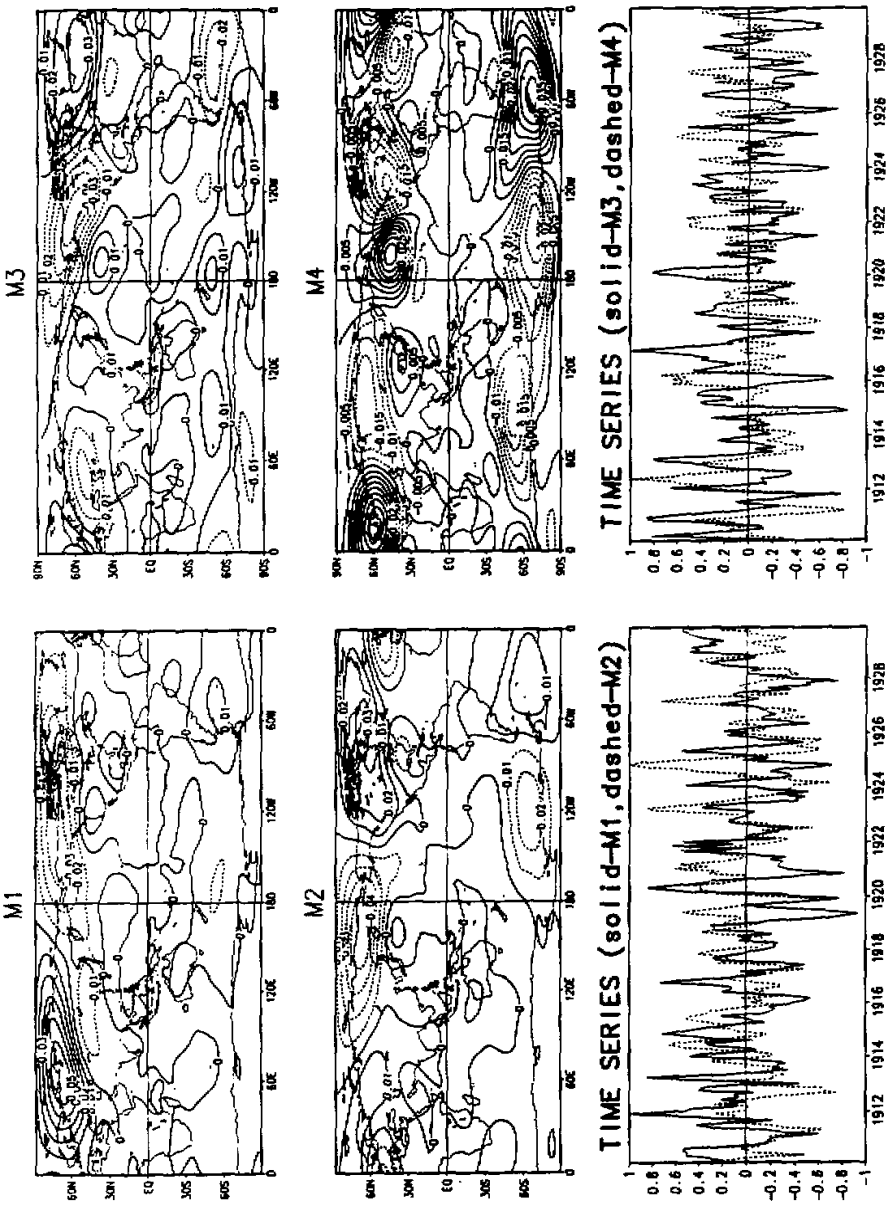

Fig. 4. The first four EOF modes of the 500 hPa eddy geopotential height for control climate experiments with respect to its own climatology. The year marks in time series plots are arbitrary, and see text for details.

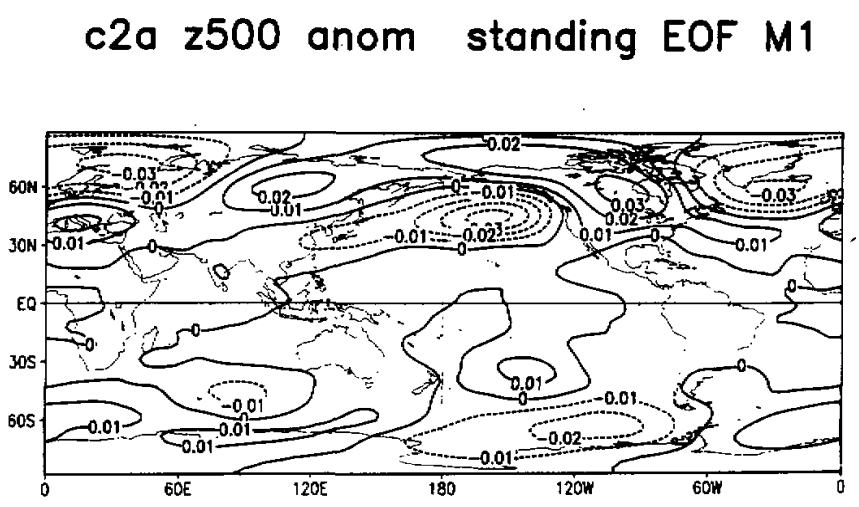

Fig. 5. The first EOF mode of the 500 hPa eddy geopotential height for control climate experiments with respect to the ensemble mean climatology.

$$\overline{SST}(x,y,t)_{warm} = \overline{SST}(x,y,t) + SST^{*}(x,y,t_0)$$
$$t = Jan.,Feb.,\cdots,Dec., \qquad t_0 = Jan.92$$

where SST is the climatology and SST* is the anomalies of Jan. 1992. Using the SST anomalies of Jan. 1989, the cold SST climatology is similarly defined as:

$$\overline{SST}(x,y,t)_{cold} = \overline{SST}(x,y,t) + SST^{*}(x,y,t_0)$$
$$t = Jan.,Feb.,\cdots,Dec., \qquad t_0 = Jan.89.$$

The SST anomalies for both Jan. 89 and Jan. 92 are shown in Fig. 6. It is worth to emphasize that both anomalies are added onto SST climatology as a constant field. Therefore, both warm and cold SST climatologies can be considered as altered climatological forcing of atmosphere under ENSO and cold events conditions, which is a major factor to modify climatological mean states of the atmosphere.

First, we computed the difference in the 500 hPa geopotential heights between warm and cold climate simulations (i.e., $Z_{CW}-Z_{CC}$) forced by warm and cold SST climatologies, respectively. And then EOF analyses were performed on the standing components of the difference ($Z_{CW}-Z_{CC}$) field. The first dominant mode and its temporal evolution are shown in Fig. 7. It is evident that wavetrain pattern and antisymmetric feature, as seen in Fig. 2b and Fig. 5, are clear in the spatial loading (Fig. 7a). The temporal evolution of the mode (Fig. 7b) is dominated by seasonality. This tells once again that the wavetrain modes in these two simulations are due to difference in their climatologies. Anomalies of either warm or cold climate simulations with respect to their own climatology show no sign of the wavetrain patterns (figure not shown). Therefore, persistent warming during ENSO and cooling during cold events in tropical central-eastern Pacific (Fig.6) give rise to the wavetrain mode in Pacific / America sector by modifying the climatological structure of stationary wave. This is

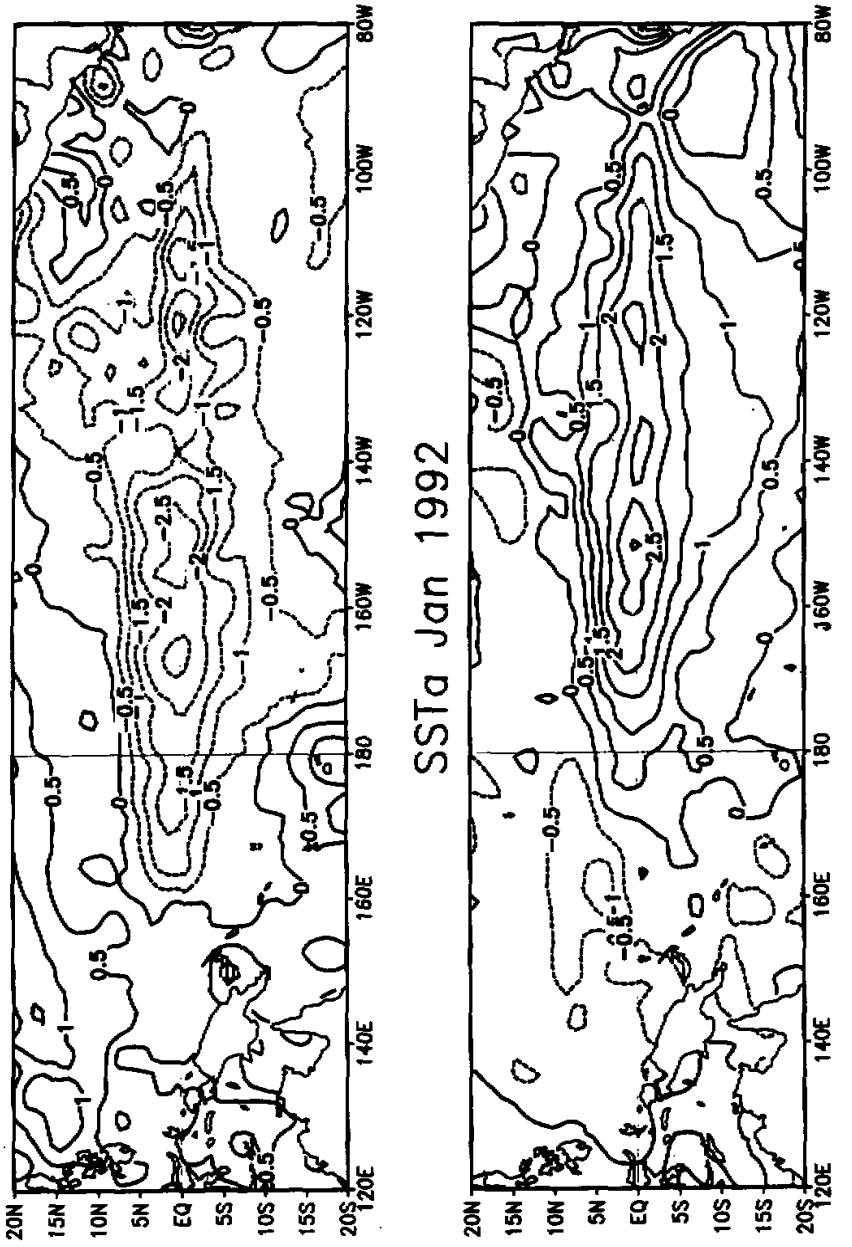

Fig. 6. SST anomalies for Jan. 1989 and Jan. 1992. Unit is °C.

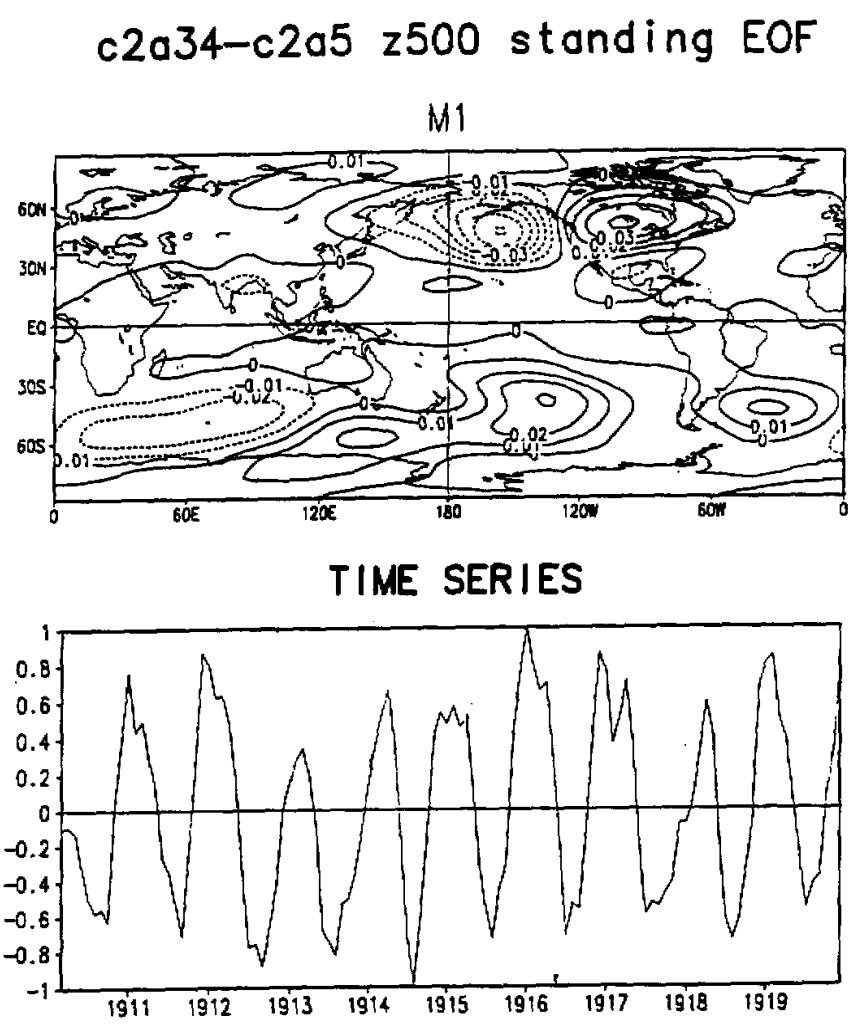

Fig. 7. The first EOF mode of the 500 hPa eddy geopotential height differences between warm climate runs and cold climate runs. The year marks are arbitrary in time series plot.

clearly shown in differences of climatological stationary wave component between warm and cold climate simulations (Fig. 8). During the Northern winter (Fig. 8a), the wavetrain is much stronger in the Northern Hemisphere than in the Southern Hemisphere corresponding to tropical anomalous heating. The reversal is true for the Northern summer (Fig. 8b). In these two seasons, both the symmetric component (as seen in Fig. 2a) and the antisymmetric component (as seen in Fig. 2b) of the wavetrain are evident, indicating that both direct response of tropical heating and its seasonal modulation are important. During transition seasons (Fig. 8c and 8d), the antisymmetric component is much weaker, reflecting less impact of seasonality.

3. *Perpetual Experiments*

Results from control and altered climate experiments point to importance of climatology. Persistent SST warming in the Pacific modifies structure of climatological stationary wave, which in turn provides favorable conditions for exciting and persisting wavetrain modes. The wavetrain modes are also modulated by the annual cycle. In this framework, the rule of tropical heating in maintaining climatological stationary wave pattern is emphasized. To further elucidate linkage between tropical heating and basic state, three perpetual experiments were performed.

The first experiment is forced by climatological January SST, the second one is forced by SST field of January 1992, and the last is forced by SST of January 1989. All experiments run for seventy months. Shown in Fig. 10 are differences of time mean stationary waves for Z_{PN}, Z_{PW}, and Z_{PC}, respectively. It is clear that the wavetrains are very well presented in all difference maps, indicating a strong relationship between tropical heating field and stationary wave structure in basic states. That is, persistent boundary forcing during ENSO (Jan. 1992) or cold (Jan. 1989) events is to modify the climatological structure of stationary wave. This altered basic state (climatological January condition) gives rise to preferred excitation of the wavetrain modes which is intrinsic in internal dynamics. This results is consistent with the climate experiments presented in previous section.

4. *Climatology vs Wavetrains*

The evidences presented above demonstrate a relationship between persistent tropical heating and changes of steady state for extratropical circulations. By recognizing the importance of mean stationary wave structures in interpretation of the wavetrains, one must then answer why the tropical SST forcing is important in changes of climatological mean states and how it impacts. To address the point and related issue of interaction between SST–forcing and climatological mean state, a root mean square of difference of the climatology between the warm climate runs and the control climate runs is computed. This quantity (Fig. 9a) measures a shift of the climatology due to warmer SST forcing as shown in Fig. 6b. The same calculation is repeated for the cold climate run to estimate the climatological changes (Fig. 9b) due to colder SST forcing as shown in Fig. 6a.

It is clear from Fig. 9a and 9b that the climatological changes due to nearly symmetric SST anomalous forcing (Fig. 6) are very different in both spatial distribution and magnitude. The changes due to the warmer SST forcing (Fig. 9a) have much larger amplitude in the PNA and PSA wavetrain regions while the changes due to the colder SST forcing (Fig. 9b) have large zonal symmetric component. This indicates that the warm SST climatology favors the wavetrain development while the colder one gives rise to uniformed enhancement of midlatitude storm activity.

A ratio of these two RMS measures is shown in Fig. 9c with greater than unit being shaded. If the departures from control climate due to the warmer and the colder SST forcings were symmetric and similar, the ratio in Fig. 9c should be close to uniform and near unit everywhere. However, values in Fig. 9c are predominantly larger than one. The global mean value of the ratio in Fig. 9c is 1.74, reflecting a fact that the mean climate changes due to the

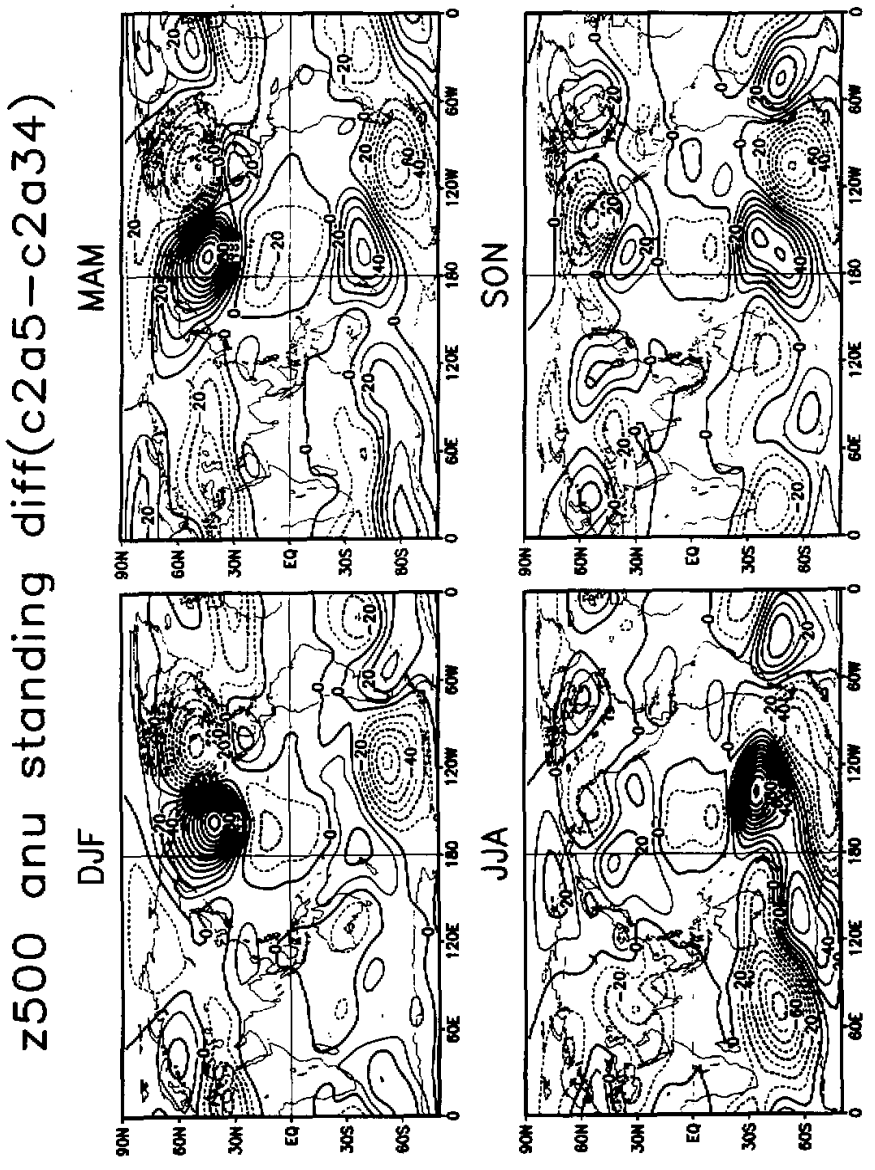

Fig. 8. Seasonal means of the 500 hPa eddy geopotential height difference between the warm climate runs and cold climate runs. Intervals are 10 m and negatives are dashed.

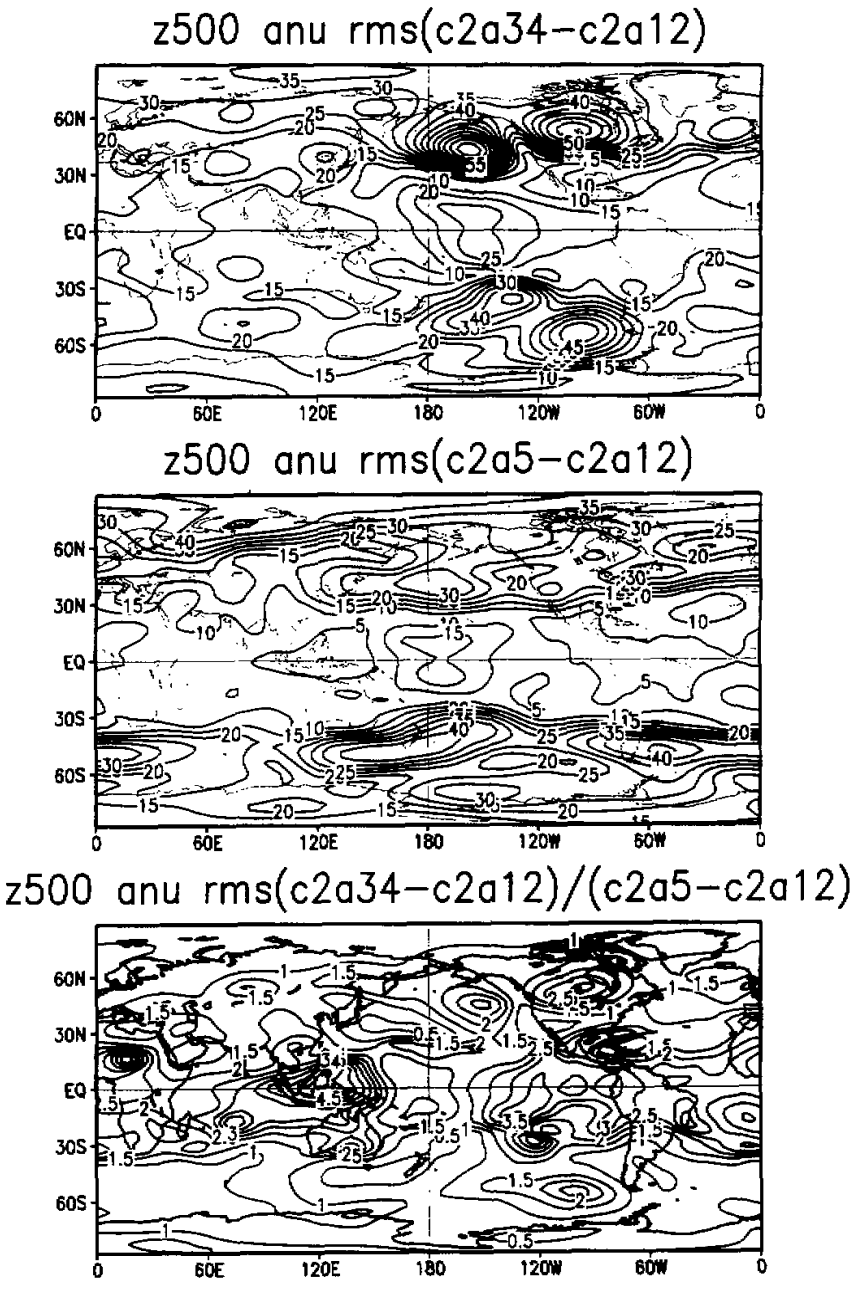

Fig. 9(a).Root mean square of the annual cycle difference between the warm climate runs and the control climate runs, (b) Root mean square of the annual cycle difference between the cold climate runs and the control climate runs, and (c) the ratio between (a) and (b) with greater than unit shaded. Intervals are 5 m in (a) and (b) and are 0.5 in (c).

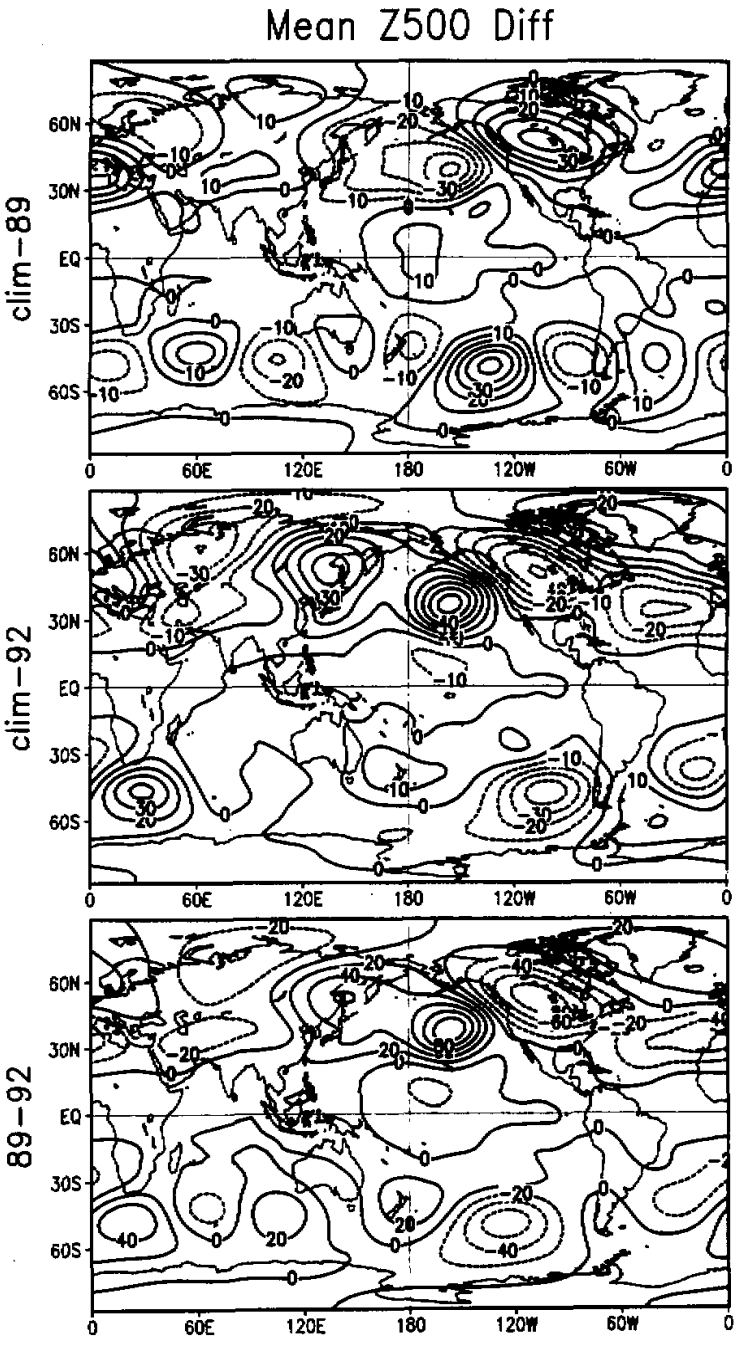

Fig. 10(a).Time mean differences between the climatological January perpetual and the cold January perpetual, (b) time mean differences between the climatological January perpetual and the warm January perpetual, and (c) time mean differences between the warm January perpetual and the cold January perpetual. Intervals are 10 m in (a) and (b) and are 20 m in (c). The negative values are dashed.

warmer SST forcing are 70 percent stronger (in the linear sense) than the one due to the colder SST forcing in global domain. Over PNA region, the ratio of the ENSO impact vs the cold event impact goes as high as three times. The high ratio regions are also found over warm pool and tropical eastern Pacific–America area. The lower ratio (less than unit) regions are generally found over mid–high latitudes of both hemispheres.

Recall that the positive and the negative SST anomalies being added onto SST climatology are nearly mirror images. This reveals simply a truth that in modifying the mean climate structures the impact of an ENSO warm event is much stronger than the one of cold events. Due to this fact, climatology of the simulation forced with observed SSTs is biased towards ENSO climatology, even if the SST series contains same amount of ENSO and cold events. This result is strongly supported by observations (Chen and van den Dool, 1995).

V. DISCUSSIONS AND CONCLUSIONS

Using the NCEP climate model, we performed a series of experiments to examine the impact of tropical SST forcing vs internal dynamics on circulation anomalies over North America region. Our focus was placed on commonly observed wavetrain patterns in Pacific–America sector, such as PNA, PSA, and TNH. The model is able to reproduce large–scale low–frequency circulation features of observation with observed SST forcing. Some important results are summarized and synthesized here with emphasis on interactions between the annual cycle and anomalies.

1. *Climatological state changes vs anomalies*

The dominant climate signals over Pacific–America region are the wavetrain patterns–the manifestation of warm and cold events (Fig. 2). However, those wavetrains appear also in non–ENSO time and are intrinsic to internal dynamics (Fig. 4). The key question addressed in this study is how the wavetrain modes intrinsic to internal dynamics can also be the predominant ENSO anomalies. In the control climate experiments ($\mathbf{CLIM}_{\mathrm{CNTL}}$), if anomalies are calculated with respect to its own climatology, the wavetrain modes exist but are not the most dominant ones of the anomalies which are resulted from internal dynamics. However, if anomalies are calculated with respect to the nine–member ensemble climatology of ensemble simulations (**ENSM**) the wavetrain modes are the most dominant ones of the anomalies (Fig. 5). This tells a fact that the climatology forced by climatological SST is different from the one forced by observed SST, even in multi–member ensembles. This is due to nonlinear interactions between SST forcing and internal dynamics of the mean stationary waves. Hence, the so–called control climatology is modified due to the presence of time–dependent SST anomalies and due to asymmetric impact of persistent and strong boundary forcing on mean climate states. In other words, there are interactions between climatological mean states and anomalous forcing. If one persists anomalous SST forcing, such as that in warm or cold events period, the climatological mean states are changed from the control climatology. This climatological mean state changes (Fig. 8) show the same structure as the wavetrain modes during ENSO and cold events (Fig. 2).

By synthesis of the above results, it is argued that persistent anomalous SST forcing during warm and cold events modifies the climatological mean stationary wave structure which

appears as an anomaly by taking the difference from mean climatology forced without anomalous SST forcing. On the other hand, the altered climatological structures influence favorable selection and / or excitation of internal wavetrain modes as shown in Fig. 4d and 4e. For warm SST anomalies (ENSO case), the modified mean climate state favors the wavetrain modes, while in cold event, the altered climatology suppresses the wavetrain modes (Chen and van den Dool, 1995). Under such a framework, it is very important to recognize the fact that the long-term mean climatology is different from either the climatology of warm events or the one of cold events (Mo and Wang, 1995). In this paper, role of SST forcing in adjusting and maintaining climatological mean stationary wave structure is emphasized.

2. *Implications for climate prediction*

Two modes of Fig. 2 describe different aspects of the wavetrain modes. The mode 1 is symmetric to equator and shows obvious tropical origin while the mode 2 is antisymmetric to equator and shows no sign of tropical forcing. Considering the results from control and altered climate experiments (Fig. 7–9) as well as perpetual experiments (Fig. 10), the mode 1 describes the mean difference of stationary wave structure between climate base state and base state of ENSO or cold events. The mode 2 reflects both seasonality of altered mean stationary wave during ENSO and cold events and intrinsic wavetrain modes during non-ENSO time. Combination of these two modes gives not only the canonical features of ENSO and cold events but also the specific characteristics of individual episode. This implies that the mode 1, due to its tropical connection and longer persistence, may be more predictable given SST forcing, while the mode 2, due to its lack of tropical connection and its linkage to internal dynamics, may be more unpredictable. This is in agreement with conclusions of Wang et al. (1995).

3. *Concluding Remarks*

By summarizing presented results, it is argued that ENSO anomalies, i.e., wavetrain patterns, over Pacific-North America region appear to be a result of modification for climatological mean stationary wave by tropical SST forcing. In this argument, the role of SST forcing in maintaining climate basic state is emphasized. It is fundamental to acknowledge the difference between traditional defined long-term mean climatology and climatology of ENSO or cold events. ENSO anomalies manifest itself as difference in climate basic states forced by strong and persistent tropical SST anomaly. Hence, so-called anomalous wavetrain modes are embedded in altered climatological mean stationary wave structures. In this regard, climatological stationary waves and its relationship to SST forcing could be crucial in understanding ENSO anomalies over Pacific-North America region.

REFERENCES

Bjerknes, J. (1966), A possible response of the atmospheric Hadley circulation to equatorial anomalies of ocean temperature, *Tellus*, **18**: 820–829.

--------, (1969), Atmospheric teleconnections from the equatorial Pacific, *Mon. Wea. Rev.*, **97**: 526–535.

Branstator, G. W. (1985a), Analysis of general circulation model sea-surface temperature anomaly simulations using a linear model, Part I: Forced solutions, *J. Atmos. Sci.*, **42**: 2225–2241.

Branstator, G.W. (1985b), Analysis of general circulation model sea-surface temperature anomaly simulations using

a linear model, Part II: Eigenvalue problems, *J. Atmos. Sci.*, **42**: 2242–2260.

Chen, W.Y. and H.M. van den Dool (1995), Low-frequency variabilities for widely different basic flows, *Tellus*, **47A**: 526–540.

Dickey, J.O., S.L. Marcus, and R. Hide (1992), Global propagation of interannual fluctuations in atmospheric angular momentum, *Nature*, **357**: 484–488.

Green, J.S.A. (1977), The weather during July (1976), Some dynamical considerations of the drought, *Weather*, **32**: 120–125.

Held, I.M., S.W. Lyons, and S. Nigam (1989), Transients and the extratropical response to El-Nino, *J. Atmos. Sci.*, **46**: 163–174.

Hoerling, M.P., M.L. Blackmon, M. Ting (1992), Simulating the atmospheric response to the 1985–87 El-Nino cycle, *J. Climate*, **5**: 669–682.

Horel, J.D., and J.M. Wallace (1981), Planetary scale atmospheric phenomena associated with the Southern Oscillation, *Mon. Wea. Rev.*, **109**: 813–829.

Hoskins, B.J., and D.J. Karoly (1981), The steady linear response of a spherical atmosphere to thermal and orographic forcing, *J. Atmos. Sci.*, **38**: 1179–1196.

Hoskins, B.J., and P.D. Sardeshmukh (1987), A diagnostic study of the dynamics of the Northern Hemisphere winter of 1985–86, *Quart. J. Roy. Meteor. Soc.*, **113**: 759–778.

Kok, C.J. and J.D. Opsteegh (1985), Possible causes of anomalies in seasonal- mean circulation patterns during the 1982–83 El Nino event, *J. Atmos. Sci.*, **42**: 677–694.

Kumar, A., M.P. Hoerling, M.Ji, A. Leetmaa, and P.D. Sardeshmukh (1994), Assessing a GCM's Suitability for making seasonal predictions, *J. Climate*..

Kumar, A., and M.P. Hoerling (1995), Prospects and limitations of seasonal atmospheric GCM predictions, *Bull Amer. Meteor. Soc.*, **76**: 335–345.

Lau, N.C. (1981), A diagnostic study of recurrent meteorological anomalies in a 15-year simulation with a GFDL general circulation model, *Mon. Wea. Rev.*, **109**: 2287–2311.

Lau, N.C. (1988), Variability in the observed midlatitude storm tracks in relation to low-frequency changes in the circulation patterns, *J. Atmos. Sci.*, **45**: 2718–2743.

Mo, K. C., and X. L. Wang (1995), Sensitivity of the systematic error of extended range forecasts to sea surface temperature anomalies, *J. Climate*, **8**: 1533–1543.

Molteni, F., L. Ferranti, T.N. Palmer, and P. Viterbo (1993), A dynamical interpretation of the global response to equatorial Pacific SST anomalies, *J. Climate*, **6**: 777–795.

Palmer, T.N. (1993), Extended-range atmospheric prediction and the Lorenz model, *Bull. Amer. Meteor. Soc.*, **74**: 49–65.

Ropelewski, C., and M. Halpert (1987), Global and regional scale precipitation patterns associated with the El Nino / Southern Oscillation, *Mon. Wea. Rev.*, **115**: 1606–1626.

Rosen, R.D. (1993), The axial momentum balance of Earth and its fluid envelope, *Surveys in Geophysics*, **14**: 1–29.

Simmons, A.J., J. M. Wallace, and G.W. Brastator (1983), Barotropic wave propagation and instability, and atmospheric teleconnection pattern, *J. Atmos. Sci.*, **40**: 1363–1392.

Smith, T.M., R.W. Reynolds, and R.E. Livezey (1995), Reconstruction of historical sea surface temperatures using empirical orthogonal functions, *J. Climate*.,

Ting, M., and M.P. Hoerling (1993), Dynamics of stationary wave anomalies during the 1986 / 87 El Nino, *Climate Dynamics*, **9**: 147–164.

--------, and P.D. Sardeshmukh (1993), Factors determining the extratropical response to equatorial diabetic heating anomalies, *J. Atmos. Sci.*, **50**: 907–918.

Shutts, G. J. (1986), A case study of eddy forcing during an Atlantic blocking episode, *Advances in Geophysics, Academic Press*, **29**: 135–162.

van Loon, H., and R.A. Madden (1981), The Southern Oscillation, Part I: Global associations with pressure and temperature in northern winter, *Mon. Wea. Rev.*, **109**: 1150–1162.

Yarnal, B., and H.F. Diaz (1986), Relationship between extremes of the Southern Oscillation and the winter climate of the Anglo–American Pacific coast, *J. Climatol.*, **6**: 197–219.

Wang, X.L., H.L. Rui, and C.F. Ropelewski (1996), An assessment of NCEP climate model–prospects and limitations of climate prediction (to appear).